

MYELOID NEOPLASIA

Iron is a modifier of the phenotypes of *JAK2*-mutant myeloproliferative neoplasms

Jan Stetka,^{1,2} Marc Usart,¹ Lucia Kubovcakova,¹ Shivam Rai,¹ Tata Nageswara Rao,¹ Joshua Sutter,¹ Hui Hao-Shen,¹ Stefan Dirnhofer,³ Florian Geier,^{1,4} Michael S. Bader,⁵ Jakob R. Passweg,⁵ Vania Manolova,⁶ Franz Dürrenberger,⁶ Nouraz Ahmed,⁷ Timm Schroeder,⁷ Tomas Ganz,⁸ Elizabeta Nemeth,⁸ Laura Silvestri,^{9,10} Antonella Nai,^{9,10} Clara Camaschella,⁹ and Radek C. Skoda¹

¹Experimental Hematology, Department of Biomedicine, University Hospital Basel and University of Basel, Basel, Switzerland; ²Department of Biology, Faculty of Medicine and Dentistry, Palacky University, Olomouc, Czech Republic; ³Institute of Medical Genetics and Pathology, University Hospital Basel, Basel, Switzerland; ⁴Swiss Institute of Bioinformatics, Basel, Switzerland; ⁵Division of Hematology, University Hospital Basel, Basel, Switzerland; ⁶CSL Vifor, St. Gallen, Switzerland; ⁷Department of Biosystems Science and Engineering, Eidgenössische Technische Hochschule Zurich, Basel, Switzerland; ⁸David Geffen School of Medicine, University of California, Los Angeles, Los Angeles, CA; ⁹Division of Genetics and Cell Biology, San Raffaele Scientific Institute, Milan, Italy; and ¹⁰Vita Salute San Raffaele University, Milan, Italy

KEY POINTS

- Iron availability alters the phenotype of MPN mouse models by affecting the lineage bias of bipotent megakaryocyte-erythroid progenitors.
- The ferroportin inhibitor vamifeport and the minihepcidin PR73-normalized hematocrit and hemoglobin levels in mouse models of PV.

***JAK2*-V617F mutation causes myeloproliferative neoplasms (MPNs) that can manifest as polycythemia vera (PV), essential thrombocythemia (ET), or primary myelofibrosis. At diagnosis, patients with PV already exhibited iron deficiency, whereas patients with ET had normal iron stores. We examined the influence of iron availability on MPN phenotype in mice expressing *JAK2*-V617F and in mice expressing *JAK2* with an *N542-E543del* mutation in exon 12 (*E12*). At baseline, on a control diet, all *JAK2*-mutant mouse models with a PV-like phenotype displayed iron deficiency, although *E12* mice maintained more iron for augmented erythropoiesis than *JAK2*-V617F mutant mice. In contrast, *JAK2*-V617F mutant mice with an ET-like phenotype had normal iron stores comparable with that of wild-type (*WT*) mice. On a low-iron diet, *JAK2*-mutant mice and *WT* controls increased platelet production at the expense of erythrocytes. Mice with a PV phenotype responded to parenteral iron injections by decreasing platelet counts and further increasing hemoglobin and hematocrit, whereas no changes were observed in *WT* controls. Alterations of iron availability primarily affected the pre-megakaryocyte-erythrocyte progenitors, which constitute the iron-responsive stage of hematopoiesis in *JAK2*-mutant mice. The orally administered ferroportin inhibitor vamifeport and the minihepcidin PR73 normalized hematocrit and hemoglobin levels in *JAK2*-V617F and *E12* mutant mouse models of PV, suggesting that ferroportin inhibitors and minihepcidins could be used in the treatment for patients with PV.**

Introduction

Myeloproliferative neoplasms (MPNs) are clonal disorders of hematopoietic stem cells (HSCs) driven by gain-of-function mutations in *JAK2*, *MPL*, or *CALR* genes.¹⁻⁷ Additional mutations that modify the course of the disease have also been described in genes involved in epigenome regulation, DNA damage response, Ras signaling, and inflammation.⁸ In patients with MPN having *JAK2*-V617F mutation, the disease can manifest as polycythemia vera (PV) with significant expansion of erythropoiesis, essential thrombocythemia (ET) with increased production of megakaryocytes and platelets, or primary myelofibrosis with extramedullary hematopoiesis.^{9,10} In contrast, patients with MPN having mutations in *JAK2* exon 12 (*E12*) invariably display a PV phenotype with predominant erythrocytosis.^{11,12}

In healthy individuals, ~80% of circulating iron is consumed for hemoglobin production, and iron availability strongly affects erythropoiesis.¹³ To maintain the high hemoglobin levels in PV, the iron regulatory peptide hepcidin that inhibits iron absorption in the gut and recycling from macrophages has to be suppressed.¹⁴ This process is partially mediated by erythroferrone,¹⁵ which is released from erythroblasts upon stimulation by erythropoietin (Epo). Erythroferrone inhibits hepcidin expression by sequestering the bone morphogenetic proteins (BMPs), which signal to increase *hepcidin* (*HAMP*) transcription.^{16,17} Mobilization of iron does not occur equally in all MPNs. Previous data in MPN animal models showed that hepcidin suppression and iron acquisition are more effective in mice with *JAK2* *E12* mutation compared with that in mice with *JAK2*-V617F mutation.¹⁸ Limiting iron availability via phlebotomy is a standard

therapy to lower hematocrit in low-risk PV.¹⁹ Iron deficiency can promote thrombocytosis.^{20,21} Reducing iron availability by exogenous administration of hepcidin mimetics that inhibit the iron transporter ferroportin is currently being investigated for the treatment of PV.^{22,23}

Here, we examined the effects of iron restriction and iron overload on MPN phenotypes in mice with *JAK2* mutation. We also investigated whether the ferroportin inhibitor vamiportin²⁴ and the minihepcidin PR73 can normalize hematocrit and hemoglobin in mouse models of PV.²⁵

Materials and methods

Patients with MPN

Blood samples and clinical data of patients with MPN were collected at the Basel University Hospital, Basel, Switzerland. Blood samples from healthy controls were obtained from the local blood donation center (Stiftung Blutspendezentrum SRK beider Basel). The study was approved by the local ethics committees (Ethik Kommission Beider Basel). Written informed consent was obtained from all patients, in accordance with the Declaration of Helsinki. The diagnosis of MPN was established based on the World Health Organization classification of myeloid neoplasms and acute leukemia.¹⁰ Information on the diagnosis and gene mutations of patients with MPN included in this study are specified in supplemental Table 1 and supplemental Methods, which are available on the *Blood* website. Additional methods are also described in supplemental Methods.

Mice

We used conditional *JAK2*-V617F transgenic "flip-flop" (*FF1*) mice,²⁶ *JAK2* E12 mutant mice (*JAK2*-N542-E543del),¹⁸ and *Jak2*-V617F knockin mice,²⁷ which were crossed with tamoxifen-inducible *ScfCre*^{ER(estrogen receptor)} mice.²⁸ The *Cre*^{ER} protein in double-transgenic *ScfCre*^{ER};*FF1* mice (*FF*_{Scf}) and *ScfCre*^{ER};*Jak2*-V617F knockin mice (*Ki*) was then activated by intraperitoneal injection of 2 mg tamoxifen (Sigma-Aldrich) for 5 consecutive days, resulting in a PV phenotype that developed within ~3 to 4 weeks.^{27,29} Alternatively, the *FF1* transgene was activated by crossing *FF*_{Scf} with *VavCre* mice,³⁰ and the resulting *VavCre*;*FF1* mice (*FF*_{Vav}) display an ET-like phenotype.²⁶ *Ki* and *E12* mice were also crossed with the *UBC-GFP* strain that express the green fluorescent protein reporter gene in all hematopoietic lineages.³¹ All mice used in this study were from pure C57BL/6N background and were maintained under specific pathogen-free conditions and in accordance with Swiss federal regulations.

Low-iron diet and iron injections

The normal mouse diet used in our facility contains 200 mg/kg iron (Kliba Nafag). To induce iron deficiency, mice were placed on a low-iron diet (iron content <5 mg iron per kg, SAFE, U8958), or on a control diet supplemented with 200 mg/kg carbonyl-iron (SAFE, U8959). Additional phlebotomies (200 μ L every 2 weeks) were performed in some mice to accentuate iron deficiency. Iron-dextran (D8517, Sigma-Aldrich) was injected intraperitoneally (250 mg/kg per mouse) for iron supplementation.

Inhibitor studies

Vamiportin (CSL Vifor) in 0.5% methylcellulose (Sigma-Aldrich) was gavaged twice a day at 100 mg/kg.³² PR73 was dissolved in

SL220 (NOF Corp) and injected intraperitoneally at 10 mg/kg twice per week.^{33,34} Control mice were injected twice a week with the solvent SL220 or gavaged twice a day with 0.5% methylcellulose.

Statistics

We used Student unpaired *t* test and one- or two-way analysis of variance with a posttest using Prism software version 8.4.3 (GraphPad Inc). Significance is denoted with asterisks: **P* < .05, ***P* < .01, ****P* < .001, and *****P* < .0001.

Results

Iron parameters and cytokine levels in patients with MPN and in MPN mouse models

We measured iron parameters in patients with MPN with *JAK2*-V617F or *JAK2* E12 mutations. Samples were taken at diagnosis before any treatment was initiated (supplemental Table 1; supplemental Methods). Patients with PV displayed higher *JAK2*-V617F variant allele fraction than patients with ET (Figure 1A), consistent with the presence of a subclone homozygous for *JAK2*-V617F,³⁵⁻³⁷ because of uniparental disomy.³⁸ Serum iron and transferrin saturation had decreased, and soluble transferrin receptor had increased in patients with PV compared with patients with the levels in ET or normal controls, and these alterations were most pronounced in patients with PV with *JAK2* E12 mutations (Figure 1A). Accordingly, hepcidin and Epo levels had decreased, and erythroferrone levels increased in patients with PV (Figure 1B). Thus, patients with PV displayed erythrocytosis and were iron deficient at diagnosis, before any treatment was initiated.³⁹ In contrast, most patients with ET with *JAK2*-V617F had normal iron parameters at diagnosis, indicating that iron availability was not limiting their potential to augment erythropoiesis.

To examine the effects of iron on the MPN phenotype, we first compared blood counts and iron parameters of *JAK2*-mutant MPN mouse models at baseline on a normal diet. We included 3 models with various degrees of PV-like phenotypes (*Ki*, *FF*_{Scf}, and *E12*)^{18,26,27} and 1 with ET-like phenotype (*FF*_{Vav}).²⁶ All PV models showed erythrocytosis and increased platelet count, except *E12* mice, whose platelets were decreased. *FF*_{Vav} mice showed thrombocytosis with normal red blood cell parameters (Figure 2A). Liver iron concentration had greatly decreased in *Ki* mice and moderately decreased in *FF*_{Scf} mice, whereas *E12* mice showed only a nonsignificant trend toward decreased liver iron (Figure 2B). *E12* mice also showed lowest levels of serum iron and transferrin saturation, similar to data from patients with PV having *JAK2* E12 mutations. Erythroferrone in all PV mice was elevated, and hepcidin levels were suppressed, most strongly in *Ki* and *E12*. In contrast, *FF*_{Vav} mice, which displayed thrombocytosis but normal hemoglobin and red blood cell parameters, displayed liver iron, erythroferrone, and hepcidin levels comparable with those in wild-type (*WT*) controls (Figure 2B). Purified populations of hematopoietic stem and progenitor cells (HSPCs) from *Ki* and *E12* mice showed increased messenger RNA (mRNA) expression of genes favoring augmented iron supply for erythropoiesis (Figure 2C). In this respect, *E12* mice showed higher expression levels of *Erfe*, transferrin receptor (*TfR1*), and *ferroportin* in pre-megakaryocyte-erythrocyte progenitors (pre-MegEs) compared with *Ki* mice, suggesting that the mutant *JAK2*-*E12* has an intrinsically increased propensity for the erythroid lineage and iron acquisition⁴⁰ and a

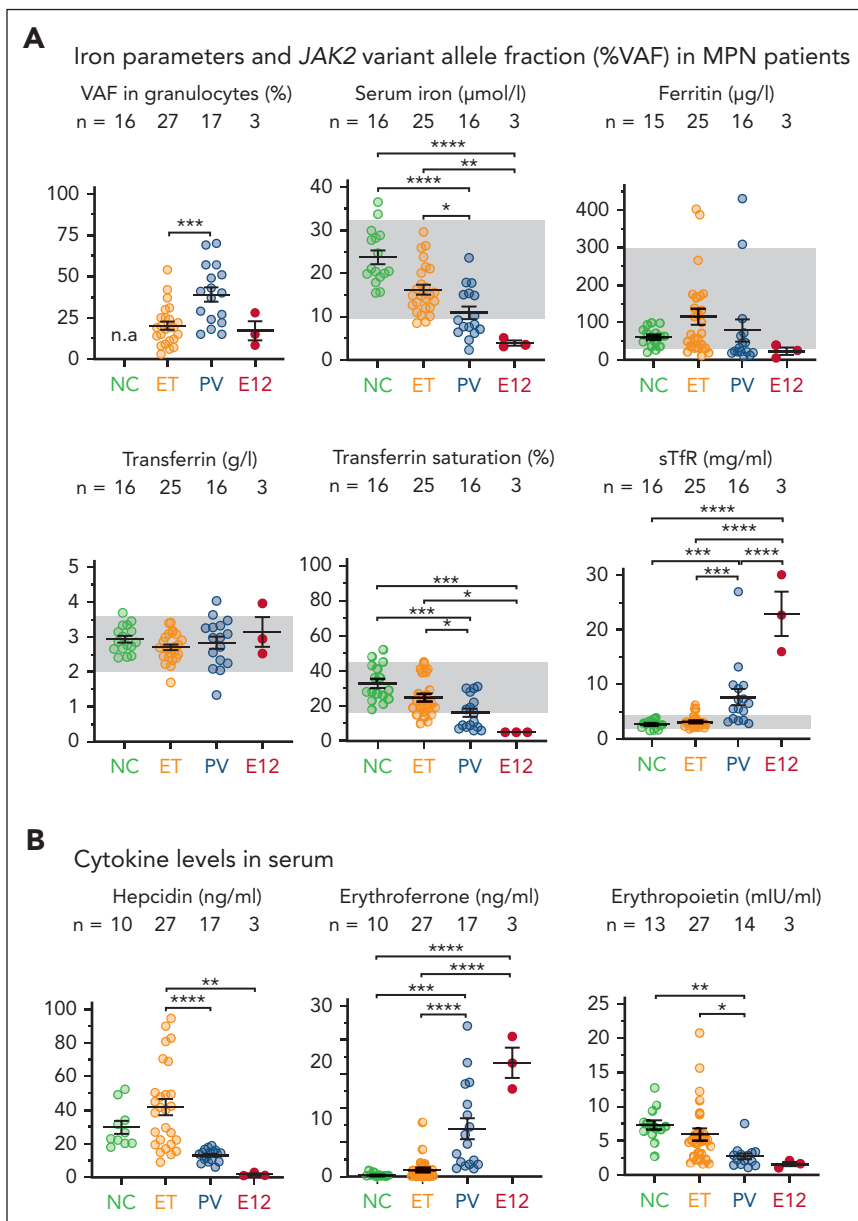


Figure 1. Status of iron parameters at the time of diagnosis in the serum of patients with MPN having mutations in JAK2 gene. (A) Iron parameters in the serum of patients with MPN at the time of diagnosis. (B) Levels of regulatory cytokines involved in iron metabolism measured in the serum of patients with MPN at the time of diagnosis. All data are presented as mean \pm standard error of the mean. Two-way analyses of variance (ANOVAs) with subsequent Tukey test were used for multiple-group comparisons. * $P < .05$; ** $P < .01$; *** $P < .001$; **** $P < .0001$. NC, normal control; sTfR, soluble transferrin receptor, VAF, variant allele frequency.

better ability to use iron for erythropoiesis.¹⁸ Based on these data, we selected *Ki* mice and *E12* mice for further studies of iron metabolism under conditions of iron restriction and iron overload.

Iron deficiency increased thrombopoiesis at the expense of erythropoiesis

To obtain enough mice for the different treatment groups, we performed transplantation of *WT* C57BL/6 recipient mice with bone marrow (BM) from *Ki*, *E12*, or *WT* mice (Figure 3A; supplemental Figure 1A). Four weeks after transplantation, recipient mice were randomized and placed on a low-iron diet, with or without phlebotomy, or on a control diet (Figure 3A). Already before start of treatment, *Ki* and *E12* mice displayed lower body weight (Figure 3B) and nonfasting glucose levels

than *WT* controls (supplemental Figure 1B), consistent with the previously described augmented energy demand of hyperactive erythropoiesis.⁴¹ Splenomegaly was reduced by a low-iron diet with or without phlebotomy in both *E12* and *Ki* mice (supplemental Figure 2). An inverse correlation with hemoglobin levels was noted in *Ki* mice (supplemental Figure 2B), suggesting increased removal of erythrocytes via hypersplenism.

Platelet counts and megakaryocyte numbers of *WT*, *E12*, and *Ki* mice increased on the low-iron diet compared with the control diet, and this increase was further accentuated via additional phlebotomy (Figure 3-D). Tpo concentrations in BM and serum were elevated in *E12* mice at baseline and inversely correlated with platelet and megakaryocyte counts in all genotypes (Figure 3D);

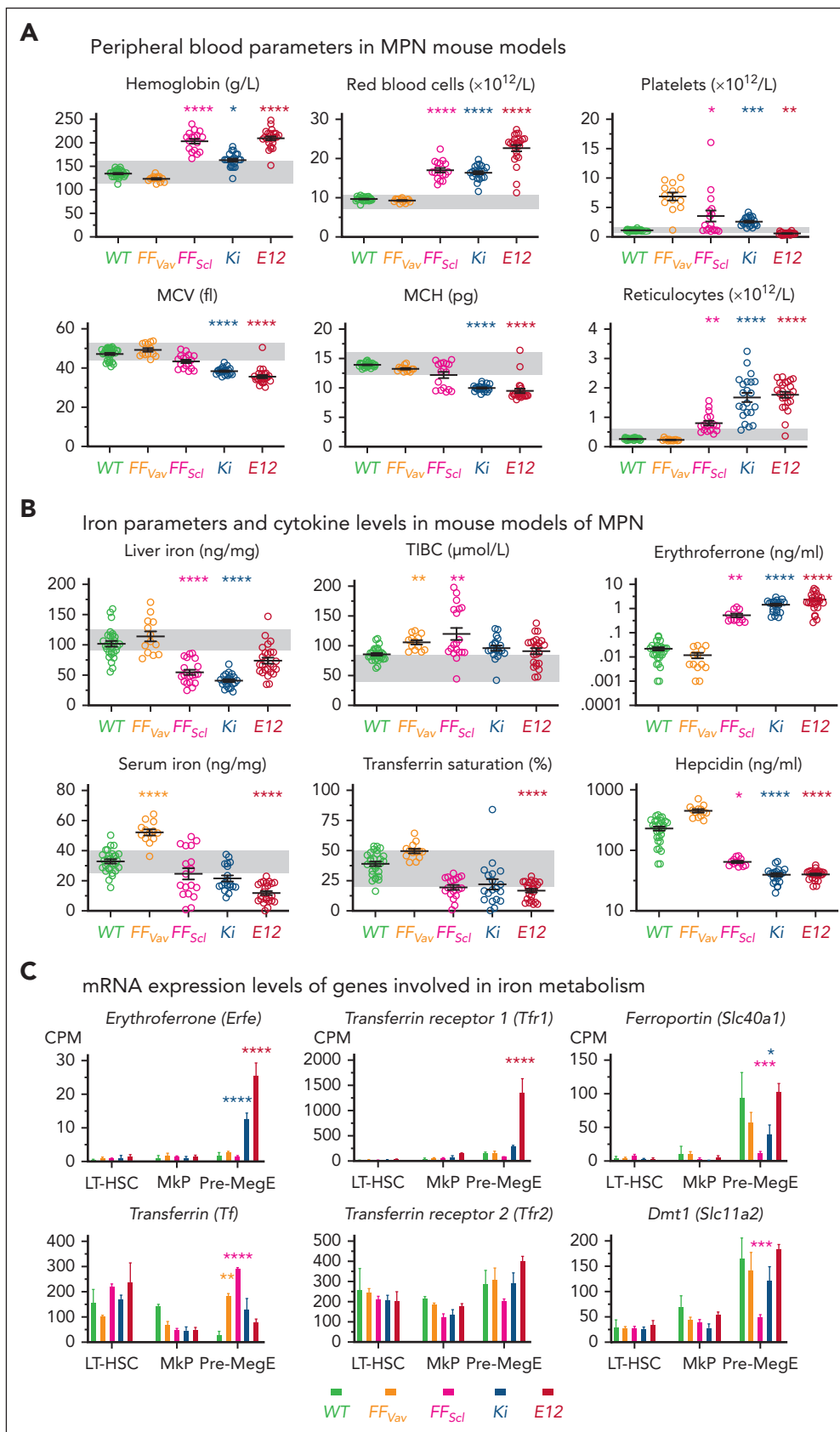
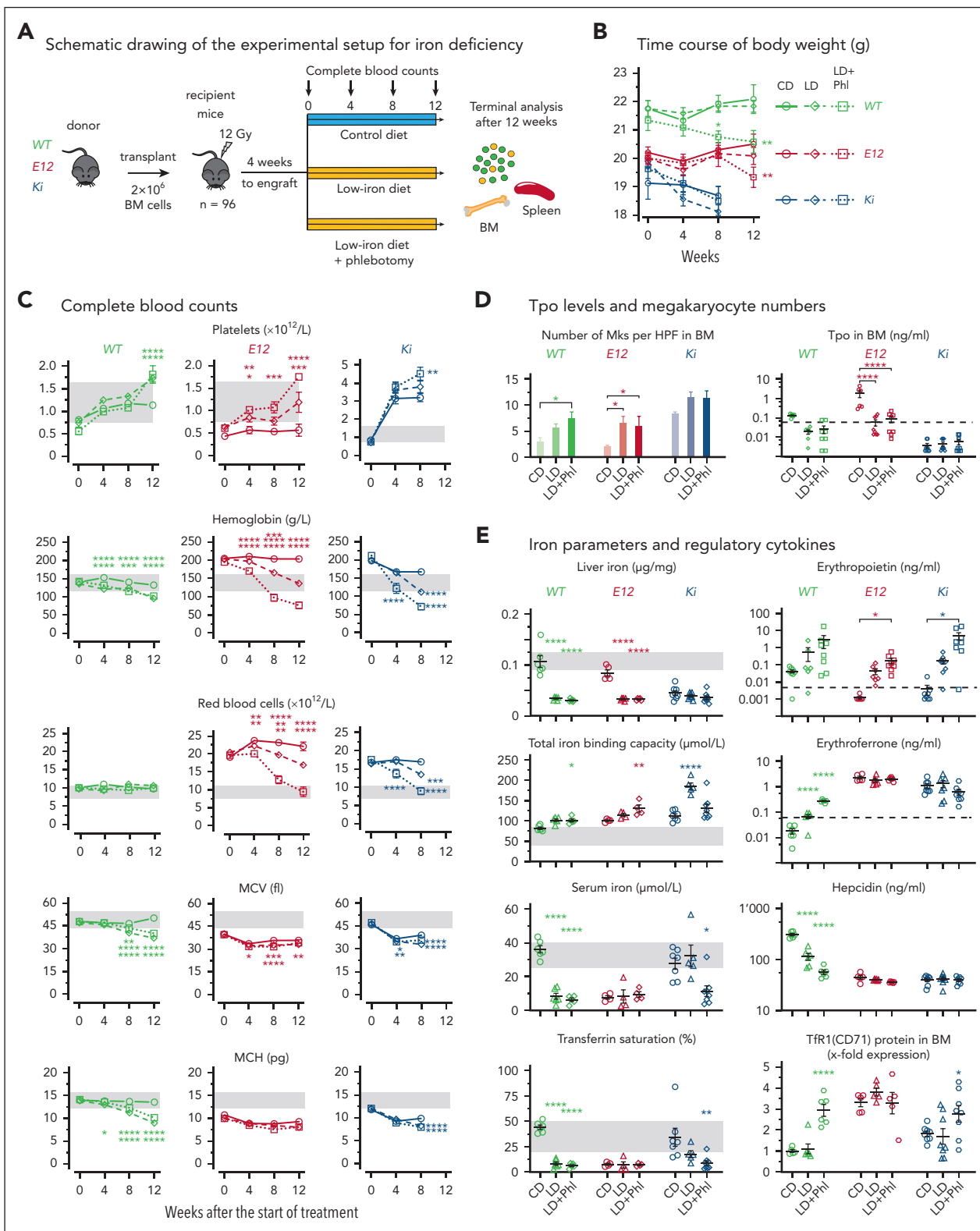


Figure 2. Iron parameters in MPN mouse models with mutations in *JAK2* gene. (A) Blood cell parameters of different MPN mouse models. (B) Iron parameters and cytokine levels in serum. Note that logarithmic scales are used for iron regulatory cytokines (erythroferrone and hepcidin). (C) RNA sequencing–derived mRNA expression levels of genes involved in iron homeostasis in hematopoietic progenitors. All data are presented as mean \pm standard error of the mean. Two-way ANOVAs with subsequent Tukey or Dunnett test were used for multiple-group comparisons. * $P < .05$; ** $P < .01$; *** $P < .001$; **** $P < .0001$. MkPs, megakaryocyte progenitors.



supplemental Figure 1C-D). Grade of BM reticulin fibrosis increased in *Ki* mice on a low-iron diet with phlebotomy (supplemental Figure 1E), consistent with the role of augmented megakaryopoiesis and increased platelet counts in myelofibrosis.^{42,43}

Mice on a low-iron diet also showed the expected decrease in red blood cell parameters (Figure 3C; supplemental Figure 1F). Anemia developed in all genotypes on a low-iron diet plus phlebotomies, most notably in *Ki* mice, which had to be euthanized prematurely after 8 weeks because they looked ill. *E12* mice on a control diet reached the highest hemoglobin values, were more resistant to iron deficiency, and, after 8 weeks, maintained higher hemoglobin levels compared with *Ki*. Mean corpuscular volume (MCV) and mean corpuscular hemoglobin (MCH) both decreased when the mice were exposed to a low-iron diet plus phlebotomy, although these were already very low with a normal diet (Figure 3C). No significant changes were found in white blood cell counts (supplemental Figure 1G).

Iron parameters and regulatory cytokines are shown in Figure 3E. Low-iron diet reduced liver iron in *E12* and *WT* mice, whereas stores were already exhausted at baseline in *Ki* mice. Serum iron in *E12* mice, already low with the control diet, did not decrease further with a low-iron diet with or without phlebotomy, whereas serum iron and transferrin saturation in *Ki* mice decreased only when they were on a low-iron diet plus phlebotomy, accompanied by an increase in total iron binding capacity. As expected for PV, serum Epo levels were low and suppressed in *E12* and *Ki* mice when on a control diet but increased in response to lowering hemoglobin when on a low-iron diet with or without phlebotomy. Epo transcription is primarily regulated by hypoxia-inducible factor 2 α (*Hif2a*), whose activity is controlled at the protein level by oxygen-dependent prolyl hydroxylases that initiate posttranslational degradation of HIF α subunits.⁴⁴ To estimate the activity of HIF, we assayed the mRNAs for HIF target genes *Vegfa*, *Igf2*, and *Glut1* (*Slc2a1*) and found that on a low-iron diet plus phlebotomy, their expression had increased together with Epo mRNA (supplemental Figure 3). *Erfe* and *Hamp* expression in *WT* mice responded to iron deficiency, whereas *Ki* and *E12* mice showed already maximally increased *Erfe* and suppressed *Hamp* expression when on a normal diet and did not respond further to iron deficiency (Figure 3E). Because *Erfe* is produced by erythroid progenitors as a target gene of Epo signaling, these data suggest that despite low Epo levels, hyperactive Epo receptor signaling is maintained in erythroid progenitors by the mutant *JAK2*. Consistent with the massively increased erythropoiesis, BM and spleen cells from *E12* mice showed very high cell-surface expression of TfR1 (TfR1/CD71) even with a normal diet (Figure 3E; supplemental Figure 1H).¹⁸ Overall, iron deficiency induced a reciprocal increase in platelet counts and decrease in hemoglobin levels in all genotypes and also resulted in the expected changes in proteins involved in iron homeostasis.

To determine at what stage of hematopoietic development iron deficiency influenced erythropoiesis vs thrombopoiesis, we assessed the frequencies of HSPCs in the BM and spleen (Figure 4). On a control diet, long-term HSC (LT-HSC) numbers in the BM were increased in *E12* and *Ki* mice compared with that those in *WT* (Figure 4A), and an overall increase in HSPCs was seen in the spleens from *Ki* mice compared with those from *WT*, reflecting enhanced involvement of the spleen in MPN hematopoiesis. Low-iron diet with phlebotomy decreased LT-HSCs in the spleens of *Ki* mice. Furthermore, an increase in

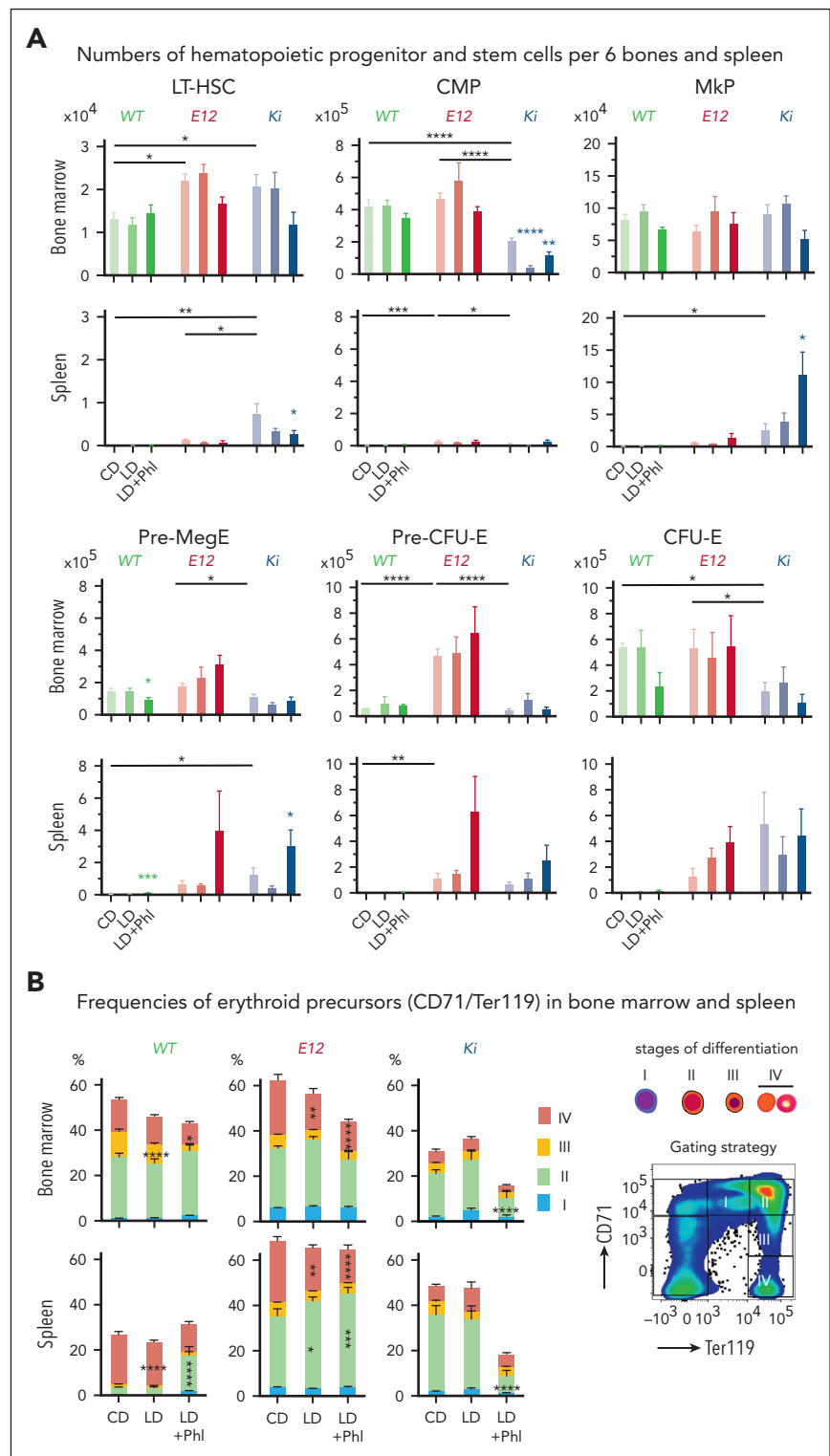
megakaryocyte progenitors and pre-MegEs was noted in the spleens of *Ki* mice, consistent with a shift toward increased megakaryopoiesis in response to iron deficiency. Analysis of late erythroid maturation stages revealed an increase in early precursors (stage II) and a decrease in late precursors (stage IV) in *E12* mice, whereas a general decrease in the numbers of erythroid precursors was observed in *Ki* mice on a low-iron diet plus phlebotomy (Figure 4B). Because pre-MegEs were reported to respond to iron deficiency, we also assessed the lineage output of single-cell-sorted pre-MegEs in liquid cultures in vitro (supplemental Figure 4). Pre-MegEs isolated from the BM of *E12* and *Ki* mice on a low-iron diet showed reduced erythroid commitment compared with mice on a control diet, whereas *WT* mice did not show this bias. Moreover, a slight increase in megakaryocytic output was found in pre-MegEs from *E12* mice on a low-iron diet. Overall, iron deficiency in *JAK2*-mutant MPN mice decreased terminal erythroid maturation and increased megakaryocyte-committed progenitors mainly in the spleen.

Parenteral iron administration increased erythropoiesis at the expense of megakaryopoiesis in mice with *JAK2*-mutated MPN

Next, we examined the effects of parenteral iron supplementation on MPN megakaryopoiesis and erythropoiesis. We again performed BM transplantations to obtain enough *JAK2*-mutant mice for analysis, and injected iron-dextran intraperitoneally into recipient mice at weeks 1 and 4 after transplantation (Figure 5A; supplemental Figure 5A). *E12* and *Ki* mice injected with iron showed weight loss (Figure 5B) were visibly impaired and had to be euthanized prematurely at 12 and 8 weeks after transplantation, respectively. Platelet counts and megakaryocyte numbers in the BM decreased by variable degrees in *E12* and *Ki*, whereas no such changes were noted in *WT* mice (Figure 5C-D). Conversely, iron-supplemented *E12* and *Ki* mice developed a stronger PV phenotype than vehicle-treated mice. Iron injections in *Ki* mice increased erythrocyte numbers, whereas in *E12* mice, they primarily raised MCV and MCH, without altering red blood cell counts (Figure 5C). No changes in red blood cell parameters were observed in *WT* mice, and white blood cells did not change after iron injections (supplemental Figure 5B). The number of megakaryocytes in the BM decreased after iron injections in *Ki* and *WT* mice (Figure 5D). Consistent with the accentuated PV phenotype, spleen weight increased after iron injections in *Ki* and *E12* mice but not in *WT* controls (Figure 5E). Thus, the decline in the general condition in *E12* and *Ki* mice correlates with the rapid increase in erythropoiesis in response to injection of iron and the more rapid decline in *Ki* mice is likely because of the more profound iron deficiency of *Ki* mice at baseline on a normal diet (Figure 2).

Liver iron concentration strongly increased upon iron injections in *WT* mice, accompanied by an increase in transferrin saturation (Figure 5F). A less pronounced increase in liver iron was seen in *Ki* and *E12* mice, and serum iron and transferrin saturation decreased in *Ki* mice, reflecting augmented use due to massively increased erythropoiesis in these mice. *E12* and *Ki* mice, also showed persistently high TfR1 (CD71) protein expression on the surface of BM cells. Despite iron injections,

Figure 4. Iron-depleted MPN mice show accumulation of megakaryocyte-committed progenitors in the spleen. (A) Analysis of hematopoietic progenitor frequencies in the BM and spleen at terminal workup. Groups of 4 to 8 mice per genotype and treatment were analyzed. (B) Analysis of erythroid maturation. Frequencies of the erythroid maturation stages in the BM and spleen are shown for individual genotypes ($n = 4-8$ mice per genotype and treatment). All data are presented as mean \pm standard error of the mean. Two-way ANOVAs with subsequent Dunnett posttest were used for multiple-group comparisons. * $P < .05$; ** $P < .01$; *** $P < .001$; **** $P < .0001$. CFU-E, colony-forming unit erythroid.



erythropoietin remained very high in *E12* and *Ki* mice, but a trend toward higher hepcidin in response to iron injections was noted, consistent with previous data showing that erythropoietin is unable to fully suppress hepcidin when the BMP pathway is activated by high iron or by deletion of *Tmprss6*, a

negative regulator of the BMP signaling.⁴⁵ Thus, parenteral iron administration lowered platelets and increased hemoglobin in *E12* and *Ki* mice, which displayed iron deficiency at baseline, whereas iron injections had no effect in *WT* mice with adequate iron stores before the injections.

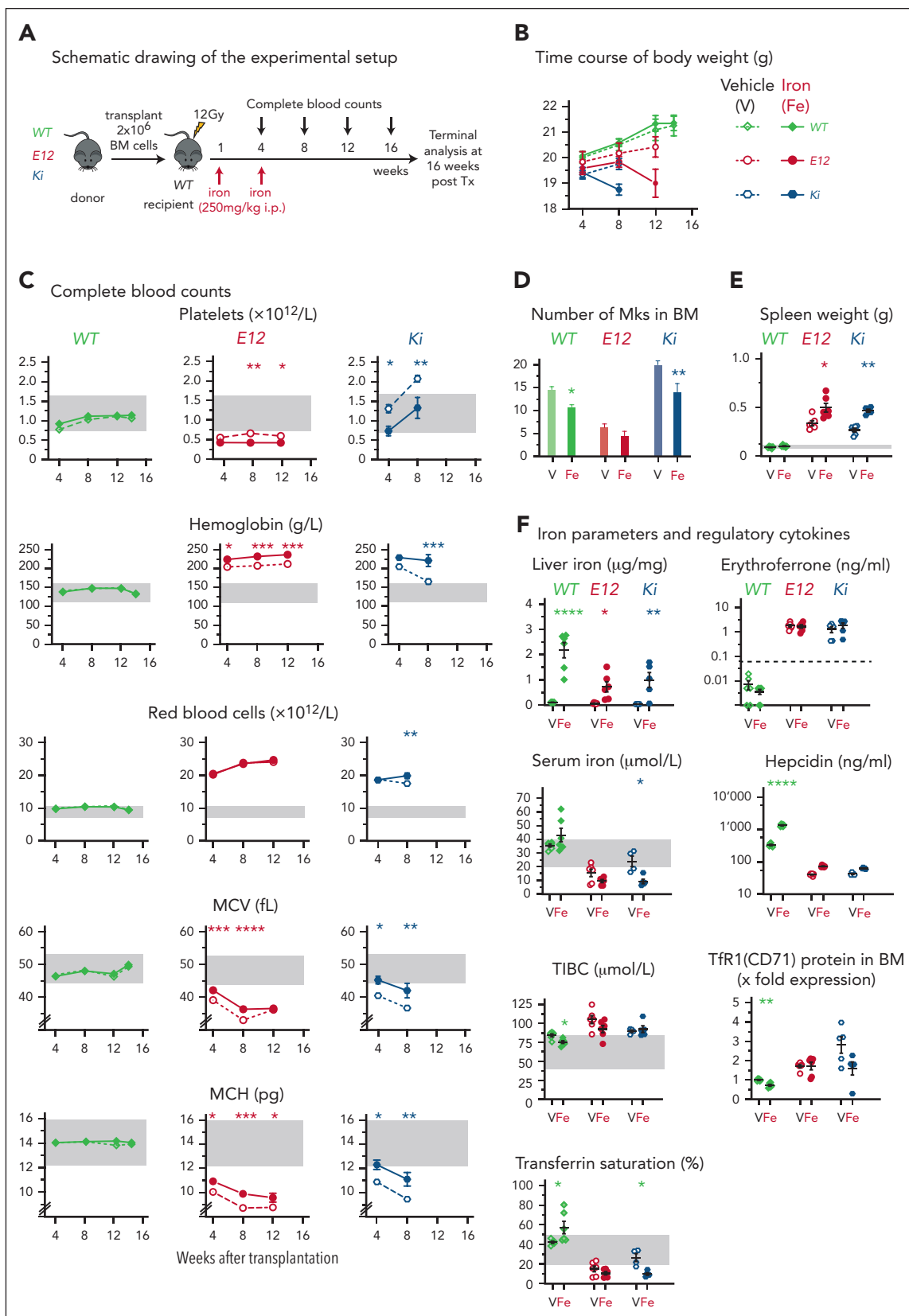


Figure 5. Effects of parenteral iron injections on MPN phenotype. (A) Schematic drawing of the experimental setup for BM transplantations and iron injections. (B) Time course of body weight ($n = 6-8$ mice per group). (C) Complete blood counts of recipient mice ($n = 6-8$ mice per group) are shown at the indicated times. (D) Numbers of Mks per 10 HPFs counted in sternum sections of mice at original magnification $\times 400$; $n = 3$ mice per genotype and treatment group. (E) Spleen weight at terminal analysis. (F) Iron parameters and regulatory cytokines at terminal analysis. Note that logarithmic scales are used for iron regulatory cytokines (erythroferrone and hepcidin). Group size was $n = 4$ to 8 mice per genotype and treatment group. Erythroferrone and hepcidin levels (shown on logarithmic scale) together with total iron binding capacity (TIBC) and transferrin saturation were determined in serum. All data are presented as mean \pm standard error of the mean. Two-way ANOVAs with subsequent Dunnett posttest or Sidak posttest were used. One-way ANOVA with subsequent Tukey posttest was used to compare spleen weight (D). * $P < .05$; ** $P < .01$; *** $P < .001$; **** $P < .0001$.

Iron injections did not alter the numbers of LT-HSCs or common myeloid progenitors (CMPs) in the BM and spleen in any of the genotypes (Figure 6A). Although LT-HSCs or CMPs were largely unresponsive to iron injections, we observed changes in the erythroid and megakaryocytic progenitors. These alterations were reciprocal to the changes induced by iron deficiency (Figure 3) and were predominantly noted in the spleen. Detailed analysis of erythroid maturation (Figure 6B) showed an increase in terminally differentiated erythroid cells (stage IV) in *E12* and *Ki* mice upon iron injection, whereas no changes were observed in *WT* mice.

Collectively, these results show that in PV mouse models, iron supplementation increased hemoglobin levels at the expense of platelets production. These changes appear to operate mainly through the pre-MegE stage, which responded to iron restriction with an increase in platelet production at the expense of red blood cells in all models. In contrast, effects of increased iron supply were only observed in PV models, which, when on a normal diet at baseline, already displayed some degree of iron deficiency.

The ferroportin inhibitor vamifeport and the hepcidin agonist PR73 normalize hemoglobin levels in 2 PV mouse models

Because iron depletion via phlebotomy is a standard therapy in low-risk PV, we examined whether iron restriction through the inhibition of ferroportin-mediated export of cellular iron by vamifeport or the minihepcidin PR73 could be used to normalize hemoglobin and hematocrit in mouse models of PV.^{24,25,46,47} We performed competitive BM transplantations to obtain cohorts of mice expressing *Jak2-V617F* (*Ki*) or *JAK2-E12* (*E12*) in hematopoietic cells only (Figure 7A). After 6 weeks, recipient mice were randomized into 2 treatment groups and a control group and were then treated for 6 weeks with vamifeport by gavage (100 mg/kg twice a day) or with PR73 by intraperitoneal injections (10 mg/kg twice per week). Treatment was well tolerated and no significant changes in body weight were observed (Figure 7B). Hemoglobin normalized, and hematocrit was decreased in *E12* and *Ki* mice treated with vamifeport and PR73 compared with vehicle controls (Figure 7C). In *Ki* mice, vamifeport lowered MCV and MCH levels but did not affect erythrocyte numbers, whereas PR73 substantially reduced erythrocyte numbers but did not decrease MCH and even slightly increased MCV after 6 weeks of treatment. Platelet counts increased in *Ki* mice treated with vamifeport and, to a lesser degree, also in *E12* and *WT* mice treated with PR73.

An increase in spleen weight was noted in *E12* and *Ki* mice treated with PR73 but not in mice treated with vamifeport, whereas liver weight was not affected by any of the treatments (Figure 7D). Vamifeport and PR73 increased iron concentration in the spleen, suggesting increased retention of iron in splenic macrophages, whereas liver iron concentration was significantly increased only in *Ki* mice treated with PR73. As expected, vamifeport and PR73 lowered serum iron and transferrin saturation in all genotypes (Figure 7E). In line with decreased iron availability, PR73 in *E12* and *Ki* mice led to increased serum erythroferrone accompanied by elevated *Erfe* mRNA expression in BM erythroid cells, compatible with an increase of expression on a per cell basis. Vamifeport increased serum erythroferrone in *E12* mice only, despite unchanged *Erfe* mRNA in the BM. This increase of *Erfe* in serum is likely related to the

increased numbers of erythroblasts in the spleen of vamifeport-treated *E12* mice (supplemental Figure 6). Hepcidin decreased in *WT* mice only, and remained suppressed in *E12* and *Ki* mice.

Overall, vamifeport and PR73 showed similar efficacy to normalize hemoglobin and hematocrit in our *JAK2*-mutant mouse models of PV. Vamifeport showed the expected effects of blocking the iron exporter ferroportin with decreased MCV and MCH, whereas PR73 acted primarily by lowering erythrocyte numbers without affecting the MCV and MCH.

Discussion

Patients with PV who are untreated as well as *JAK2*-mutant mouse models with a PV-like phenotype on a control diet already exhibited iron deficiency, whereas patients with ET as well as *JAK2*-mutant mice with an ET-like phenotype (*FF_{Vav}*) had normal iron stores (Figures 1 and 2).³⁹ Low-iron diet with or without phlebotomy further increased platelet production and resulted in anemia, even in mice with PV that initially displayed marked erythrocytosis (Figure 3). In PV models with augmented erythropoiesis and preexisting low liver iron (in *Ki* and, to a lesser extent, in *E12* mice), iron injections lowered platelet counts and further increased hemoglobin production (Figure 5). In contrast, iron injections had no effect on *WT* mice, which had normal liver iron before the injections. These findings are consistent with the notion that iron overload alone, for example, in hereditary hemochromatosis, is not associated with erythrocytosis.⁴⁸ Thus, the PV phenotype in patients with PV and in PV mouse models develops while being limited by iron deficiency.

The observed iron deficiency in PV mouse models is caused by the rapid expansion of erythropoiesis, resulting in a massive increase in hematocrit and red blood cell numbers. The demand for iron leads to a decrease in serum iron, transferrin saturation, and, ultimately, reduced liver iron stores. Although increased erythroferrone and suppressed hepcidin are expected to augment intestinal iron resorption, the iron stores did not normalize over time and remained subnormal in these mice (Figure 2), despite the fact that the normal diet contains 200 mg/kg iron, which is in excess of normal iron requirements in mice. Therefore, we abstained from testing a diet supplemented with an even higher content of iron, and, instead, we used parenteral iron injections, which bypass the enteral bottleneck, deliver more iron in a shorter time, and allow us to examine how iron is distributed between the different compartments (liver, serum, and erythropoiesis in the BM and spleen).

Despite an increase in liver iron concentration, serum iron and transferrin saturation in PV mouse models was not normalized by iron injections (Figure 5), suggesting that hyperactive erythropoiesis rapidly consumed the injected iron. Considering that healthy BM consumes ~80% of circulating iron, hyperactive erythropoiesis driven by mutant *JAK2* in PV is expected to require substantially more iron.

A number of studies described HSCs with an intrinsic capacity to commit directly to the megakaryocytic lineage, thereby bypassing the pre-MegE stage,⁴⁹⁻⁵⁴ estimated to account for ~30% of megakaryopoiesis.⁵⁴ However, the relative contribution of this shortcut can be altered under stress or pathological conditions.^{55,56} HSCs

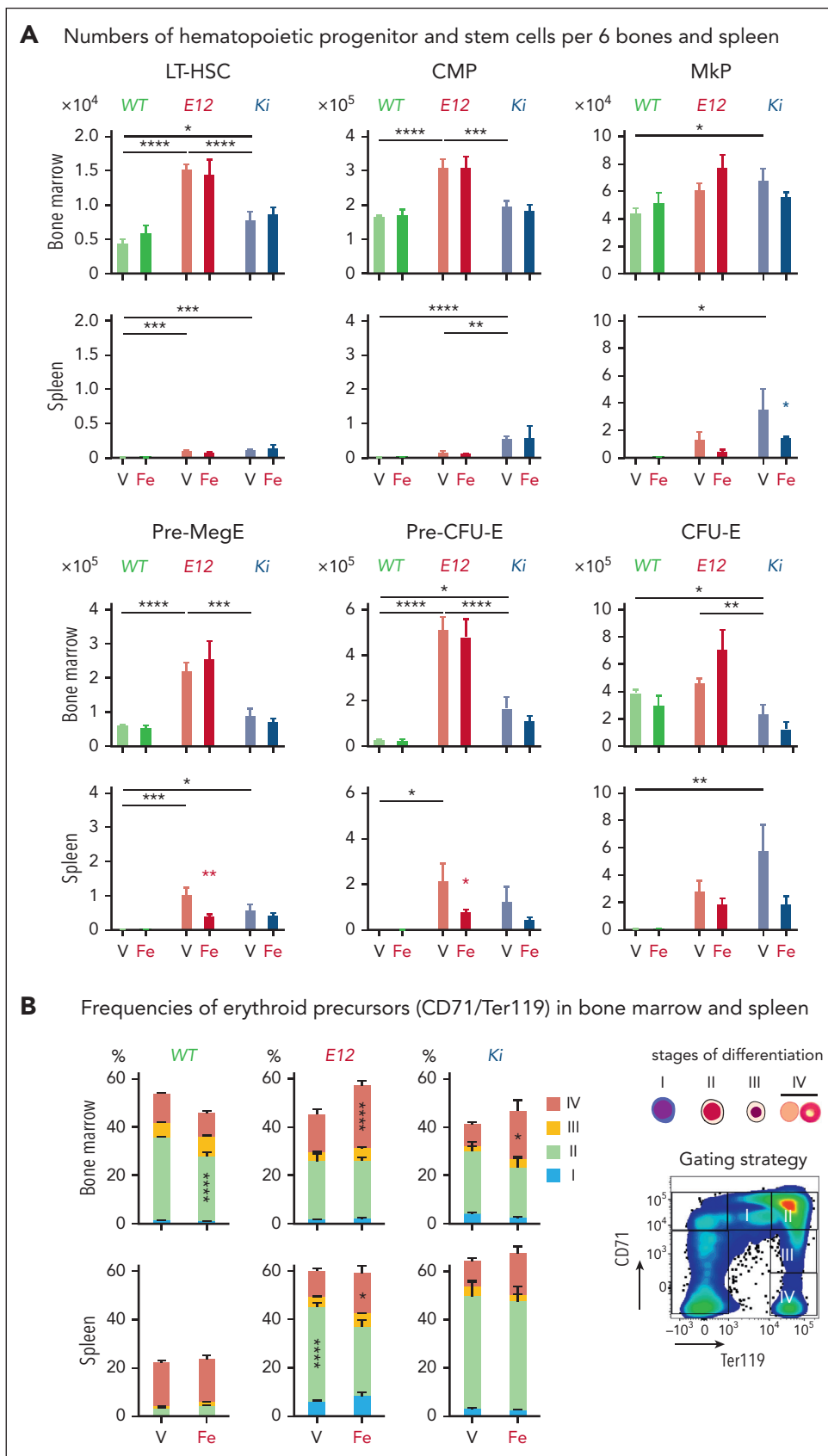


Figure 6. Effects of parenteral iron injections on hematopoietic progenitor and stem cells at terminal workup. (A) Bar graphs show frequencies of HSPCs in the BM and spleen ($n = 5-8$ mice per group). (B) Analysis of erythroid maturation ($n = 5-8$ mice per group). All data are presented as mean \pm standard error of the mean. Unpaired 2-tailed Mann-Whitney test (A) or two-way ANOVAs with Dunnett (B) posttest were used. * $P < .05$; ** $P < .01$; **** $P < .0001$.

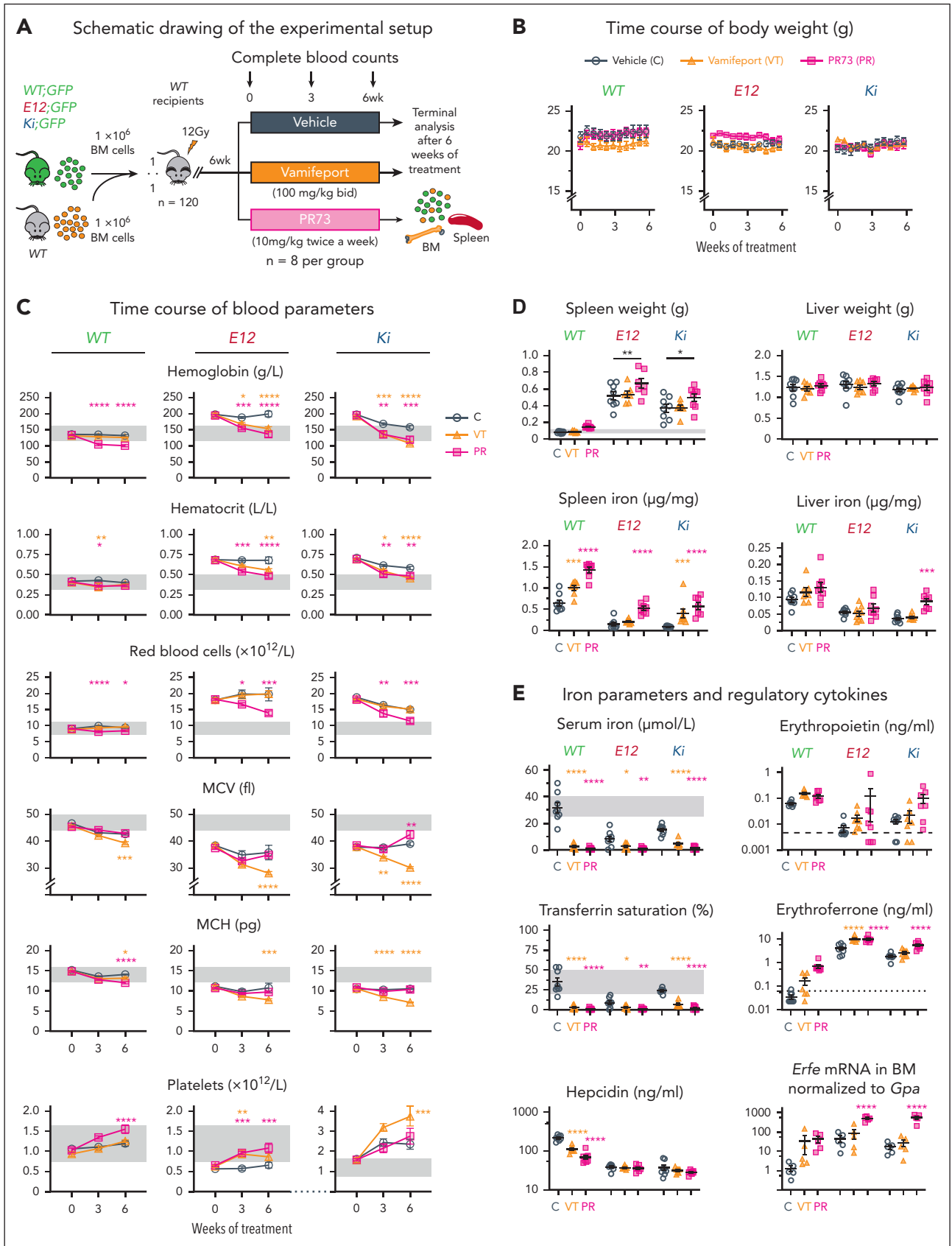


Figure 7. Effects of ferroportin inhibition on MPN phenotype in mice with PV. (A) Schematic drawing of the experimental setup for the BM transplantations and treatment with ferroportin inhibitor vamifeport and the hepcidin mimetic PR73. (B) Time course of body weight (n = 8 mice per group). (C) Complete blood counts of recipient mice (n = 8 mice per group) are shown at the indicated times. (D) Analysis of the spleen and liver at terminal workup. (Top) Spleen and liver weight, (bottom) iron concentration in the spleen and liver. (E) Iron parameters and regulatory cytokines at terminal workup. Note that logarithmic scales are used for iron regulatory cytokines (Epo, erythroferone, and

with megakaryocytic bias can be identified by increased expression of CD41,^{51,52} or a vWF-GFP reporter gene.⁵⁰ However, we did not detect changes in the percentages of the CD41^{hi} subsets of HSCs or CMPs upon inducing changes in iron availability (data not shown). In contrast, pre-MegEs and megakaryocyte progenitors increased under iron deficiency (Figure 4) and decreased after iron injections (Figure 6). Our data are consistent with the model in which pre-MegEs in WT mice having acquired iron deficiency, or in *Tmprss6*^{-/-} mice having genetic iron deficiency represented the iron-responsive stage of hematopoietic differentiation.⁵⁷ Here, we showed that pre-MegEs were also sensitive to iron deficiency in all JAK2-mutant MPN models.

The phenotype of *E12* mice with marked erythrocytosis and subnormal platelet counts appears to reflect the preference of the *E12*-mutated Jak2 protein for the EpoR over the TPO-receptor (MPL).⁴⁰ As a result, erythropoiesis through pre-MegEs is already massively augmented in *E12* mice at baseline, leading to reduced-iron stores and erythrocytosis at the expense of platelet production. Normalizing iron through injections in *E12* mice resulted in thrombocytopenia (Figure 5), suggesting that *E12* signaling is unable to stimulate the LT-HSC/CMP shortcut to megakaryopoiesis. Our findings lead to a model that integrates the properties of the different mutant JAK2 and their preference for erythropoiesis vs megakaryopoiesis and the influence of iron availability on the phenotypic expression in the MPN mouse models studied (supplemental Figure 7).

Finally, we show that reducing the availability of iron for hematopoiesis by inhibiting ferroportin with vamiport or the hepcidin agonist PR73 normalized hematocrit and hemoglobin levels in *E12* and *Ki* mouse models of PV. The differences between vamiport and PR73 in altering MCV and MCH vs erythrocyte numbers could be because of the differences in the pharmacokinetics and pharmacodynamics between the 2 compounds. The half-life of vamiport was only ~2 to 3 hours when in the rat and sustained hypoferrremia for ~4 to 8 hours.²⁴ The minihepcidin M009 (7.5 mg/kg subcutaneously) had a longer half-life and sustained hypoferrremia for >48 to 72 hours in the rat.⁴⁷ The half-life of the closely-related minihepcidin PR73 is expected to be in a similar range as that of M009. It is therefore conceivable that a more profound inhibition of ferroportin by PR73 could transiently generate sufficient iron restriction to inhibit cell division of erythroid progenitors resulting in reduced erythrocyte numbers. The current dosage of vamiport may not achieve sufficiently profound inhibition of ferroportin to interfere with cell division, therefore not affecting erythrocyte numbers. Indeed, in an earlier experiment, vamiport 100 mg/kg combined with a reduced-iron diet also decrease erythrocyte numbers (data not shown). Thus, the severity and duration of iron restriction could be the main factor determining whether erythrocyte numbers will be affected.

These results suggest that both agents are suitable candidates as an alternative to phlebotomy in the treatment of patients with PV. Indeed, rusfertide, another hepcidin agonist similar to PR73, showed promise in clinical trials.²³

Acknowledgments

The authors thank the members of the laboratory for helpful discussions and critically reading the manuscript.

This work was supported by grants from the Swiss National Science Foundation (31003A_166613 and 310030_185297) and Swiss Cancer Research Foundation (KFS-3655-02-2015 and KFS-4462-02-2018) (R.C.S.), and partially by the Ministry of Health of the Czech Republic (NV19-07-00412) (J.S.).

Authorship

Contribution: J. Stetka designed and performed research, analyzed data, and wrote the manuscript; M.U., L.K., S.R., T.N.R., H.H.-S., J. Sutter, and N.A. performed research and analyzed data; S.D., F.G., M.S.B., J.R.P., and T.S. analyzed data; V.M., F.D., T.G., E.N., L.S., A.N., and C.C. designed research and analyzed data; and R.C.S. designed research, analyzed data, and wrote the manuscript.

Conflict-of-interest disclosure: R.C.S. is a scientific adviser/scientific advisory board member, has equity in Ajax Therapeutics, and has consulted for and received honoraria from Novartis and Bristol Myers Squibb/Celgene. V.M. and F.D. are full time employees of CSL Vifor and are inventors in patents related to vamiport. T.G. and E.N. have been consultants for Vifor, are shareholders in Intrinsic LifeSciences and Solaris Pharma, and have received consulting fees from Disc Medicine, Fibrogen, AstraZeneca, Ionis Pharmaceuticals, and Rallybio. T.G. has also received consulting fees from Alnylam Pharmaceuticals, Akebia Therapeutics, Global Blood Therapeutics, Gossamer Bio, Pharmacosmos, Sierra Oncology, and Silence Therapeutics. E.N. has received consulting fees from GSK, Novo Nordisk, Protagonist, and Shield Therapeutics. The remaining authors declare no competing financial interests.

The current affiliation for T.N.R. is Stem Cells and Cancer Biology Laboratory, Department of Oncology and Hematology, Medical Research Center, Kantonsspital St. Gallen, St. Gallen, Switzerland.

ORCID profiles: J. Stetka, 0000-0003-4301-2856; T.N.R., 0000-0002-9928-5944; J. Sutter, 0000-0002-4556-8973; V.M., 0000-0002-2072-8942; T.S., 0000-0001-9320-0252; T.G., 0000-0002-2830-5469; E.N., 0000-0002-3477-2397; A.N., 0000-0002-0739-5282; C.C., 0000-0003-1427-0143; R.C.S., 0000-0002-3626-9496.

Correspondence: Radek C. Skoda, Experimental Hematology, Department of Biomedicine, University Hospital Basel and University of Basel, Hebelstrasse 20, 4031 Basel, Switzerland; email: radek.skoda@unibas.ch.

Footnotes

Submitted 1 August 2022; accepted 6 February 2023; prepublished online on *Blood* First Edition 9 February 2023. <https://doi.org/10.1182/blood.2022017976>.

RNA sequencing data reported in this article have been deposited in the Gene Expression Omnibus database (accession number GSE184254).

Data and information about the reagents are available on request from the corresponding author, Radek C. Skoda (radek.skoda@unibas.ch).

The online version of this article contains a data supplement.

There is a [Blood Commentary](#) on this article in this issue.

The publication costs of this article were defrayed in part by page charge payment. Therefore, and solely to indicate this fact, this article is hereby marked "advertisement" in accordance with 18 USC section 1734.

Figure 7 (continued) hepcidin). All data are presented as mean ± standard error of the mean. One- and two-way ANOVA with subsequent Dunnett posttest were used. **P* < .05; ***P* < .01; ****P* < .001; *****P* < .0001.

REFERENCES

- James C, Ugo V, Le Couedic JP, et al. A unique clonal JAK2 mutation leading to constitutive signalling causes polycythaemia vera. *Nature*. 2005;434(7037):1144-1148.
- Kralovics R, Passamonti F, Buser AS, et al. A gain-of-function mutation of JAK2 in myeloproliferative disorders. *N Engl J Med*. 2005;352(17):1779-1790.
- Levine RL, Wadleigh M, Cools J, et al. Activating mutation in the tyrosine kinase JAK2 in polycythemia vera, essential thrombocythemia, and myeloid metaplasia with myelofibrosis. *Cancer Cell*. 2005;7(4):387-397.
- Baxter EJ, Scott LM, Campbell PJ, et al. Acquired mutation of the tyrosine kinase JAK2 in human myeloproliferative disorders. *Lancet*. 2005;365(9464):1054-1061.
- Klampfl T, Gisslinger H, Harutyunyan AS, et al. Somatic mutations of calreticulin in myeloproliferative neoplasms. *N Engl J Med*. 2013;369(25):2379-2390.
- Nangalia J, Massie CE, Baxter EJ, et al. Somatic CALR mutations in myeloproliferative neoplasms with nonmutated JAK2. *N Engl J Med*. 2013;369(25):2391-2405.
- Pikman Y, Lee BH, Mercher T, et al. MPLW515L is a novel somatic activating mutation in myelofibrosis with myeloid metaplasia. *PLoS Med*. 2006;3(7):e270.
- Vainchenker W, Kralovics R. Genetic basis and molecular pathophysiology of classical myeloproliferative neoplasms. *Blood*. 2017;129(6):667-679.
- Levine RL, Gilliland DG. Myeloproliferative disorders. *Blood*. 2008;112(6):2190-2198.
- Arber DA, Orazi A, Hasserjian R, et al. The 2016 revision to the World Health Organization classification of myeloid neoplasms and acute leukemia. *Blood*. 2016;127(20):2391-2405.
- Scott LM, Tong W, Levine RL, et al. JAK2 exon 12 mutations in polycythemia vera and idiopathic erythrocytosis. *N Engl J Med*. 2007;356(5):459-468.
- Passamonti F, Elena C, Schnittger S, et al. Molecular and clinical features of the myeloproliferative neoplasm associated with JAK2 exon 12 mutations. *Blood*. 2011;117(10):2813-2816.
- Hentze MW, Muckenthaler MU, Galy B, Camaschella C. Two to tango: regulation of mammalian iron metabolism. *Cell*. 2010;142(1):24-38.
- Nemeth E, Tuttle MS, Powelson J, et al. Hepcidin regulates cellular iron efflux by binding to ferroportin and inducing its internalization. *Science*. 2004;306(5704):2090-2093.
- Kautz L, Jung G, Valore EV, Rivella S, Nemeth E, Ganz T. Identification of erythropoietin as an erythroid regulator of iron metabolism. *Nat Genet*. 2014;46(7):678-684.
- Arezes J, Foy N, McHugh K, et al. Erythropoietin inhibits the induction of hepcidin by BMP6. *Blood*. 2018;132(14):1473-1477.
- Lim PJ, Duarte TL, Arezes J, et al. Nr2f2 controls iron homeostasis in haemochromatosis and thalassaemia via Bmp6 and hepcidin. *Nat Metab*. 2019;1(5):519-531.
- Grisouard J, Li S, Kubovcakova L, et al. JAK2 exon 12 mutant mice display isolated erythrocytosis and changes in iron metabolism favoring increased erythropoiesis. *Blood*. 2016;128(6):839-851.
- Marchioli R, Finazzi G, Specchia G, et al. Cardiovascular events and intensity of treatment in polycythemia vera. *N Engl J Med*. 2013;368(1):22-33.
- Choi SI, Simone JV. Platelet production in experimental iron deficiency anemia. *Blood*. 1973;42(2):219-228.
- Evstatiev R, Bukaty A, Jimenez K, et al. Iron deficiency alters megakaryopoiesis and platelet phenotype independent of thrombopoietin. *Am J Hematol*. 2014;89(5):524-529.
- Casu C, Nemeth E, Rivella S. Hepcidin agonists as therapeutic tools. *Blood*. 2018;131(16):1790-1794.
- Ginzburg Y, Kirubamoorthy K, Salleh S, et al. Rusfertide (PTG-300) induction therapy rapidly achieves hematocrit control in polycythemia vera patients without the need for therapeutic phlebotomy. *Blood*. 2021;138(suppl 1):390.
- Manolova V, Nyffenegger N, Flace A, et al. Oral ferroportin inhibitor ameliorates ineffective erythropoiesis in a model of beta-thalassemia. *J Clin Invest*. 2019;130(1):491-506.
- Fung E, Chua K, Ganz T, Nemeth E, Ruchala P. Thiol-derivatized minihepcidins retain biological activity. *Bioorg Med Chem Lett*. 2015;25(4):763-766.
- Tiedt R, Hao-Shen H, Sobas MA, et al. Ratio of mutant JAK2-V617F to wild-type Jak2 determines the MPD phenotypes in transgenic mice. *Blood*. 2008;111(8):3931-3940.
- Hasan S, Lacout C, Marty C, et al. JAK2V617F expression in mice amplifies early hematopoietic cells and gives them a competitive advantage that is hampered by IFN α . *Blood*. 2013;122(8):1464-1477.
- Gothert JR, Gustin SE, Hall MA, et al. In vivo fate-tracing studies using the Scl stem cell enhancer: embryonic hematopoietic stem cells significantly contribute to adult hematopoiesis. *Blood*. 2005;105(7):2724-2732.
- Kubovcakova L, Lundberg P, Grisouard J, et al. Differential effects of hydroxyurea and INC424 on mutant allele burden and myeloproliferative phenotype in a JAK2-V617F polycythemia vera mouse model. *Blood*. 2013;121(7):1188-1199.
- de Boer J, Williams A, Skavdis G, et al. Transgenic mice with hematopoietic and lymphoid specific expression of Cre. *Eur J Immunol*. 2003;33(2):314-325.
- Schaefer BC, Schaefer ML, Kappler JW, Marrack P, Kiedl RM. Observation of antigen-dependent CD8+ T-cell/ dendritic cell interactions in vivo. *Cell Immunol*. 2001;214(2):110-122.
- Nyffenegger N, Zennadi R, Kalleda N, et al. The oral ferroportin inhibitor vamifeport improves hemodynamics in a mouse model of sickle cell disease. *Blood*. 2022;140(7):769-781.
- Preza GC, Ruchala P, Pinon R, et al. Minihepcidins are rationally designed small peptides that mimic hepcidin activity in mice and may be useful for the treatment of iron overload. *J Clin Invest*. 2011;121(12):4880-4888.
- Ramos E, Ruchala P, Goodnough JB, et al. Minihepcidins prevent iron overload in a hepcidin-deficient mouse model of severe hemochromatosis. *Blood*. 2012;120(18):3829-3836.
- Scott LM, Scott MA, Campbell PJ, Green AR. Progenitors homozygous for the V617F mutation occur in most patients with polycythemia vera, but not essential thrombocythemia. *Blood*. 2006;108(7):2435-2437.
- Li S, Kralovics R, De Libero G, Theodorides A, Gisslinger H, Skoda RC. Clonal heterogeneity in polycythemia vera patients with JAK2 exon12 and JAK2-V617F mutations. *Blood*. 2008;111(7):3863-3866.
- Godfrey AL, Chen E, Pagano F, et al. JAK2V617F homozygosity arises commonly and recurrently in PV and ET, but PV is characterized by expansion of a dominant homozygous subclone. *Blood*. 2012;120(13):2704-2707.
- Kralovics R, Guan Y, Prchal JT. Acquired uniparental disomy of chromosome 9p is a frequent stem cell defect in polycythemia vera. *Exp Hematol*. 2002;30(3):229-236.
- Ginzburg YZ, Feola M, Zimran E, Varkonyi J, Ganz T, Hoffman R. Dysregulated iron metabolism in polycythemia vera: etiology and consequences. *Leukemia*. 2018;32(10):2105-2116.
- Yao H, Ma Y, Hong Z, et al. Activating JAK2 mutants reveal cytokine receptor coupling differences that impact outcomes in myeloproliferative neoplasm. *Leukemia*. 2017;31(10):2122-2131.
- Rao TN, Hansen N, Hilfiker J, et al. JAK2-mutant hematopoietic cells display metabolic alterations that can be targeted to treat myeloproliferative neoplasms. *Blood*. 2019;134(21):1832-1846.
- Villeval JL, Cohen-Solal K, Tulliez M, et al. High thrombopoietin production by hematopoietic cells induces a fatal myeloproliferative syndrome in mice. *Blood*. 1997;90(11):4369-4383.

43. Chagraoui H, Komura E, Tulliez M, Giraudier S, Vainchenker W, Wendling F. Prominent role of TGF-beta 1 in thrombopoietin-induced myelofibrosis in mice. *Blood*. 2002;100(10):3495-3503.
44. Kaelin WG Jr, Ratcliffe PJ. Oxygen sensing by metazoans: the central role of the HIF hydroxylase pathway. *Mol Cell*. 2008;30(4):393-402.
45. Nai A, Rubio A, Campanella A, et al. Limiting hepatic Bmp-Smad signaling by matriptase-2 is required for erythropoietin-mediated hepcidin suppression in mice. *Blood*. 2016;127(19):2327-2336.
46. Chua K, Fung E, Micewicz ED, Ganz T, Nemeth E, Ruchala P. Small cyclic agonists of iron regulatory hormone hepcidin. *Bioorg Med Chem Lett*. 2015;25(21):4961-4969.
47. Casu C, Oikonomidou PR, Chen H, et al. Minihepcidin peptides as disease modifiers in mice affected by beta-thalassemia and polycythemia vera. *Blood*. 2016;128(2):265-276.
48. Barton JC, Bertoli LF, Rothenberg BE. Peripheral blood erythrocyte parameters in hemochromatosis: evidence for increased erythrocyte hemoglobin content. *J Lab Clin Med*. 2000;135(1):96-104.
49. Yamamoto R, Morita Y, Oeohara J, et al. Clonal analysis unveils self-renewing lineage-restricted progenitors generated directly from hematopoietic stem cells. *Cell*. 2013;154(5):1112-1126.
50. Sanjuan-Pla A, Macaulay IC, Jensen CT, et al. Platelet-biased stem cells reside at the apex of the haematopoietic stem-cell hierarchy. *Nature*. 2013;502(7470):232-236.
51. Gekas C, Graf T. CD41 expression marks myeloid-biased adult hematopoietic stem cells and increases with age. *Blood*. 2013;121(22):4463-4472.
52. Haas S, Hansson J, Klimmeck D, et al. Inflammation-Induced emergency megakaryopoiesis driven by hematopoietic stem cell-like megakaryocyte progenitors. *Cell Stem Cell*. 2015;17(4):422-434.
53. Nishikii H, Kanazawa Y, Umamoto T, et al. Unipotent megakaryopoietic pathway bridging hematopoietic stem cells and mature megakaryocytes. *Stem Cells*. 2015;33(7):2196-2207.
54. Rodriguez-Fraticelli AE, Wolock SL, Weinreb CS, et al. Clonal analysis of lineage fate in native haematopoiesis. *Nature*. 2018;553(7687):212-216.
55. Xavier-Ferrucio J, Krause DS. Concise review: bipotent megakaryocytic-erythroid progenitors: concepts and controversies. *Stem Cells*. 2018;36(8):1138-1145.
56. Noetzli LJ, French SL, Machlus KR. New insights into the differentiation of megakaryocytes from hematopoietic progenitors. *Arterioscler Thromb Vasc Biol*. 2019;39(7):1288-1300.
57. Xavier-Ferrucio J, Scanlon V, Li X, et al. Low iron promotes megakaryocytic commitment of megakaryocytic-erythroid progenitors in humans and mice. *Blood*. 2019;134(18):1547-1557.

© 2023 by The American Society of Hematology